



## Advanced fluorescence microscopy for *in vivo* imaging of neuronal activity

GIUSEPPE SANCATALDO,<sup>1,2</sup> LUDOVICO SILVESTRI,<sup>1,2,3</sup> ANNA LETIZIA ALLEGRA MASCARO,<sup>1,4</sup> LEONARDO SACCONI,<sup>1,3</sup> AND FRANCESCO SAVERIO PAVONE<sup>1,2,\*</sup> 

<sup>1</sup>European Laboratory for Non-Linear Spectroscopy, Via Nello Carrara, 1, 50019, Sesto Fiorentino FI, Italy

<sup>2</sup>Department of Physics and Astronomy, University of Florence, Via Giovanni Sansone, 1, 50019, Sesto Fiorentino FI, Italy

<sup>3</sup>Istituto Nazionale di Ottica, Consiglio Nazionale delle Ricerche, Largo Enrico Fermi, 6, 50125 Firenze FI, Italy

<sup>4</sup>Istituto di Neuroscienze, Consiglio Nazionale delle Ricerche, Via Giuseppe Moruzzi, 1, 56124 Pisa PI, Italy

\*Corresponding author: pavone@lens.unifi.it

Received 14 January 2019; revised 19 April 2019; accepted 21 April 2019 (Doc. ID 357632); published 31 May 2019

Brain function emerges from the coordinated activity, over time, of large neuronal populations placed in different brain regions. Understanding the relationships of these specific areas and disentangling the contributions of individual neurons to overall function remain central goals for neuroscience. In this scenario, fluorescence microscopy has been proved as the tool of choice for *in vivo* recording of brain activity. Optical advances combined with genetically encoded indicators allow a large flexibility in terms of spatiotemporal resolution and field of view while keeping invasiveness in living animals to a minimum. Here we describe the latest advancements in the field of linear and nonlinear optical microscopy with special attention to the exploration of brain functionality of model animals. The present review aims to guide the reader through the main optical systems in the field toward future directions for *in vivo* microscopy applications. © 2019 Optical Society of America under the terms of the OSA Open Access Publishing Agreement

<https://doi.org/10.1364/OPTICA.6.000758>

### 1. INTRODUCTION

Fluorescence microscopy combined with state-of-the-art indicators of neuronal activity represents the optimal tool to address brain functionality at multiple scales. From classical linear approaches to advanced optical strategies, *in vivo* optical microscopy is enabled to tackle complementary aspects of neuronal dynamics, encompassing small networks to the whole brain. The functionality of deep neurons with subcellular resolution in awake animals can now be achieved in genetically targeted populations, which seemed unattainable just a decade ago. Furthermore, recording of single neuron activity across the entire vertebrate brain discloses new insights into brain computation at the whole-organ level. Fluorescence microscopy is thus becoming the new golden standard for functional studies *in vivo*. The core of this review is a discussion on the technical advancements in linear and nonlinear optical tools applied to the investigation of brain dynamics in vertebrates. Specifically, we focus our attention to the application of functional imaging to murine and zebrafish models in order to advance toward comprehensive understanding of the human brain (Fig. 1).

We show how standard and advanced linear techniques address neuronal activity at a whole-cortex or whole-brain level, revealing spatiotemporal coordination patterns at multiple scales. Nonlinear approaches on the other side expanded the imaging capability to deep tissue while maintaining subcellular resolution. The present review aims to clarify the main optical challenges in the field and possible future directions for *in vivo* microscopy development.

### 2. LINEAR IMAGING

Neuronal activity across large scales can be best imaged using linear optical methods. Indeed, linear excitation offers the possibility to interrogate large volumes with moderate light powers, allowing imaging for long times at safe illumination doses. In this perspective, linear optical methodologies offer the unique possibility of analyzing network activity in a comprehensive and unbiased way.

#### A. Wide-Field Epifluorescence Microscopy

Even the simplest fluorescence microscopy technique—i.e., wide-field epifluorescence [Fig. 2(a)]—can provide significant insight about coordination and synchronization of different brain areas [1]. In this field, the main technological challenges are not related to the optical architecture per se but rather to novel implementations allowing brain imaging in behaviorally relevant contexts. On one hand, head-restrained systems allow recording of neural activity in mice during a resting state [1,2] or when performing easy tasks [3], maybe within a virtual reality environment [4]. On the other hand, miniaturization of the wide-field microscope allows its implantation directly onto the head of the animal, opening the possibility of functional imaging of freely behaving rodents in complex contexts [5–7] including social interaction [8]. When moving to smaller animal models, like zebrafish larvae, head-restrained wide-field imaging [9] cannot be replaced by physical implantation of the microscope on the animal's head. Besides, observation of freely moving subjects has been demonstrated by using real-time feedback systems to either move the

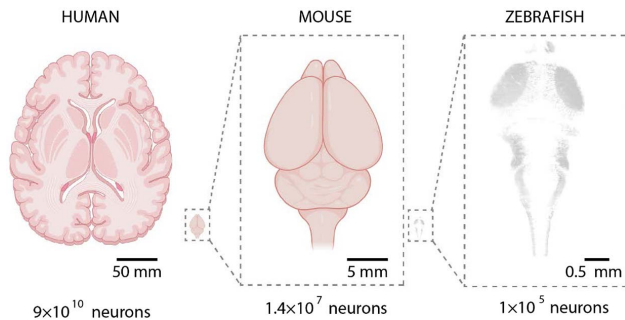


**Fig. 1.** Human, mouse, and zebrafish larvae brains. Comparison of spatial extent and number of neurons of human and vertebrate animal models.

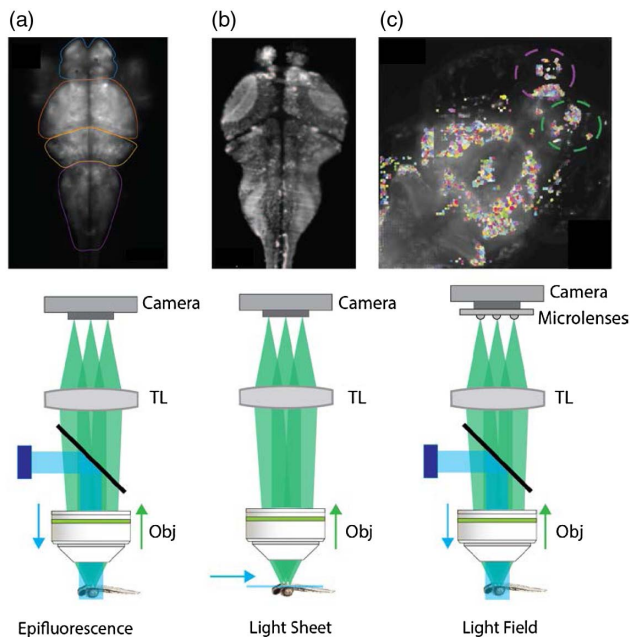


**Fig. 2.** Linear imaging of neuronal activity. (a) General scheme of epifluorescence wide-field imaging. Epifluorescence imaging of zebrafish brain, adapted by permission [9]. (b) General scheme of light-sheet fluorescence microscopy. Light-sheet imaging of zebrafish brain, adapted by permission from Springer Nature [13]. (c) General scheme of light field microscopy; application of this scheme for whole-brain functional imaging in a zebrafish larva. Adapted by permission from Springer Nature [24].

experimental platform (leaving the larva always under the microscope) [10] or to project the position of the fish onto a spatially limited detector [11].

## B. Light-Sheet Microscopy

The epifluorescence implementations mentioned above cannot provide single-cell resolution in living brains for two reasons. First, biological tissue usually scatters visible light. Second, this optical scheme inherently lacks optical sectioning, resulting in images overwhelmed by out-of-focus blur. To overcome the former limitation, transparent animal models allowing optical access to the living brain have become used more and more frequently with zebrafish larvae above all. The latter restriction can be circumvented by using

different optical schemes that allow full 3D resolution. In this respect, light-sheet microscopy [LSM, Fig. 2(b)] emerged as the method of choice, as it allows fast, high-resolution imaging of living samples with limited phototoxicity [12]. After the pioneering works of Ahrens and Panier, showing for the first time whole-brain imaging at single-cell resolution [13,14], many labs around the world worked to refine this method. In detail, a first challenge is to reduce the impact of the sample on the microscope to increase image quality; to this aim, adaptive optics has been introduced to correct specimen-induced aberrations [15]. Shadowing artefacts are another annoying problem in LSM, especially in dynamic settings; the use of self-healing Bessel beams [16], of multiple beams [17], or of diffuse light sheets [18] helps to increase image homogeneity for a true “high-fidelity” imaging. A second challenge is, conversely, to reduce the impact of the microscope onto the sample in order to perform imaging in the most natural conditions. In this respect, a practical issue is represented by the photostimulation of the larva’s eyes. To limit this problem, some special illumination geometries have been designed to limit optical stimulation of the larva’s eyes [19]. A different approach to address the same issue is two-photon LSM [20], which, however, comes at increased technical and financial costs. A further technical challenge for functional LSM is imaging speed, which is still quite slow (about 1 Hz) compared to neuronal dynamics. The main limiting factor is the need to move either the sample or the detection objective in order to scan the imaging plane across the whole brain. To overcome the need for this physical motion, extension of the depth of focus has been proposed, either by adding spherical aberration to the system [21] or by using a cubic phase mask [22]. In this way, only the weightless light sheet needs to be scanned across the sample, and the volumetric frame rate can be increased by 1 order of magnitude [21], being limited only by the signal-to-noise ratio and by camera readout speed. However, a practical limitation of these approaches is the computationally demanding post-processing, which can become the real bottleneck in an experimental pipeline.

## C. Light Field Microscopy

Despite its continuously growing popularity, LSM also presents some inherent limitations. For instance, this method requires a complex geometry in the microscope and consequently non-obvious sample mounting strategies [19]. A valid alternative method that can easily work in standard epifluorescence configurations, is light field microscopy (LFM) [23]. In this technique, the 3D structure of the specimen is extracted by recording at the image plane not only the intensity of light but also its phase. This complete reconstruction of the light field (hence the name of the technique) is possible by using a lenslet array that transforms the local inclination of light rays in a spatial displacement [Fig. 2(c)]. By solving the inverse problem of reconstructing the source distribution given the light field, it is then possible to obtain a 3D representation of the sample from a single image. LFM allows fast 3D imaging of whole zebrafish brains at almost cellular resolution [24]. Spatiotemporal resolution can be further increased by exploiting the spatiotemporal sparsity of the brain activity signal (using a compressive sensing framework [25]) or by using speckle illumination [26]. Pégard *et al.* demonstrated LFM imaging of more than 800 individual neurons in a zebrafish larva at a frame rate of 100 Hz [25], clearly demonstrating the potential of LFM for following fast neuronal dynamics in large populations. In any case, it should be noted that computational manipulation of the

signal requires additional photons to obtain robust results and signal-to-noise ratio. This penalty, besides requiring the use of a higher dose of light for imaging, fundamentally limits the dynamic range of these methods, since the same detector must collect a few “signal” photons together with many “background” photons.

#### D. Linear Microscopy in Strongly Scattering Samples

Functional linear microscopy requires substantially transparent specimens to afford cellular resolution. Thus, high-resolution analysis of the brain activity with a single photon is usually performed in small transparent animal models like zebrafish larvae. However, a few studies have reported the application of either LSM or LFM to cell-resolution functional imaging of the mammalian cortex. Holekamp and co-authors described the application of an objective-coupled LSM to monitor neurons in the mouse vomeronasal organ with cellular resolution [27]. More recently, Bouchard and colleagues introduced swept confocally aligned planar excitation (SCAPE), a variant of LSM that uses a single objective to generate an inclined light sheet and to detect fluorescent emission [28]. SCAPE has been demonstrated for functional dendritic imaging in living mice with sub-cellular resolution. However, single-photon LSM cannot penetrate more than 80–100  $\mu\text{m}$  in the mammalian brain, preventing imaging of the somas of cortical principal neurons [27,28]. A deeper penetration (up to 380  $\mu\text{m}$ ) inside the mammalian brain is instead allowed by seeded iterative demixing (SID) microscopy, a computational extension of LFM that, similarly to compressive LFM, creates a dictionary of the light field footprint of each neuron and finds the temporal evolution of the signal from each neuron by solving a least-squares non-negative minimization [29]. SID-LFM can successfully separate contributions from neurons that are at least 20  $\mu\text{m}$  away in scattering tissue, allowing extraction of activity traces from hundreds of neurons simultaneously in the mouse cortex or hippocampus. The need for higher light doses, typical of computational methods, is exacerbated in scattering samples. However, these techniques have the potential to produce experimental data that are impossible to obtain otherwise.

### 3. NONLINEAR IMAGING

In the last decades, multiphoton microscopy has been established as the method of choice for volumetric brain imaging of living animals [30,31]. Two main features characterize multiphoton microscopy. First, multiphoton excitation occurs only at the focal point, avoiding out-of-focus excitation. Second, the long-wavelength illumination light used for multiphoton excitation, usually in the near-infrared region, reduces scattering effects. These two properties permit a significant decrease in image degradation, especially when imaging is performed in deep regions of scattering samples such as a mouse brain [32]. Furthermore, because of the infrared light and the localized excitation, photo-damage and photobleaching are greatly mitigated compared to one-photon wide-field and confocal microscopy. Combined with genetically encoded activity indicators or synthetic neural indicators, multiphoton microscopy has opened a new method for functional volumetric imaging of brain activity [33–35]. However, neural events imply the need for fast optical systems that can record single-cell activity (occurring at micrometer scale) across the whole brain volume (centimeter scale). Current imaging technologies are limited by an experimental trade-off between imaging speed, field of view (FOV), and volumetric sample dimensions. In this scenario, much effort has been devoted to the development of new optical architectures that can solve or circumvent these constraints. In standard multiphoton microscopy [Fig. 3(a)], a diffraction-limited laser spot is raster scanned across a single tiny plane by the use of two moving galvanometric mirrors that control the spatial position of a pulsed laser beam in the optical path [36]. An image is formed as a well-ordered 2D sequence of points by collecting the fluorescence by a single detector (i.e., a photomultiplier tube or an avalanche photodiode), whose temporal signal is mapped to the corresponding raster-scanned point. Volumetric imaging is obtained, as a straightforward extension, by merging a stack of images acquired by translating the focal plane along the axial direction. Although such a widespread system allows light to be shined on a great number of relevant brain

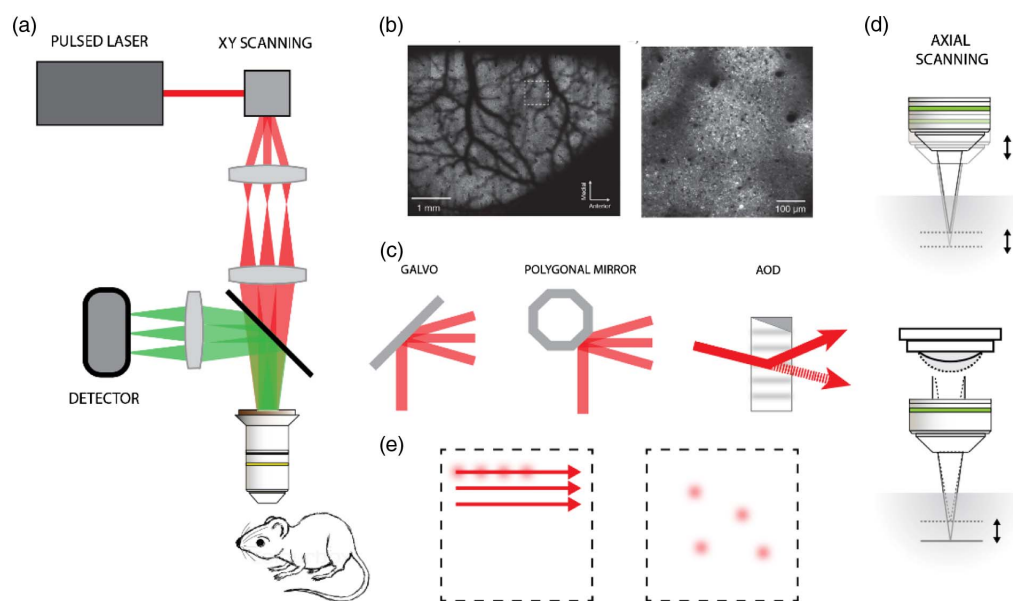


**Fig. 3.** (a) Optical layout of a two-photon laser-scanning microscope. (b) Large-FOV microscope, adapted with permission [37]. (c) Systems for beam scanning: galvo mirrors, polygonal mirrors, and acousto-optic deflectors. (d) Axial scanning: (top) linear stage system, (bottom) ETL-focus shifting. (e) AOD random-access imaging of selected neurons.

processes, it suffers by a limited imaging area (FOV) and by a slow volumetric imaging speed. These are severely limiting constraints since brain activity relies on fast interactions between large populations of neurons located in different brain regions. Understanding the relationships between these specific areas and disentangling the contributions of individual neurons to circuit function is an essential step for deciphering brain functioning.

### A. Large Field of View

Typical two-photon microscopes equipped with off-the-shelf objectives provide high resolution (sub-micrometer resolution) and deep imaging but have FOVs that are smaller than a millimeter and dramatically fail when fast imaging across a large area is required. Large-FOV imaging may be performed by a low magnification objective but it comes at the cost of a low NA and therefore of a poor spatial resolution. To connect the activity recording of single cells to large-area imaging, specially designed optics or optimization of the standard system are necessary. A microscope able to perform mesoscale imaging with subcellular resolution across the whole cortex has been developed by custom-designed lenses and an optimized scanning system [Fig. 3(b)] [37]. A subcellular resolution (lateral  $0.66\ \mu\text{m}$ , axial  $4.09\ \mu\text{m}$ , NA 0.6) over an extended volume (diameter  $5\ \text{mm} \times 1\ \text{mm}$ ) has been reported. Alternative strategies to achieve a large FOV are based on the accurate combination of off-the-shelf components that avoids the design and production of highly customized optic elements. Based on commercial components, a large FOV two-photon microscope has been presented by Kleinfeld's group [38]. The optical system is designed to minimize aberrations within the scan path that significantly degrade the resolution. The microscope is able to image the full extent of a mouse cortex with a spatial resolution limited by the objective (ranging from  $1.2\ \mu\text{m}$  at the center of the FOV to a  $1.5 \times 2.0\ \mu\text{m}$  ellipse at the edge of the field) across an  $8\ \text{mm} \times 10\ \text{mm}$  field. Despite the non-uniform resolution, imaging was successfully demonstrated for the analysis of mesoscopic neurovascular dynamics across cortical hemispheres without the need to stitch smaller FOVs. On the same principle of using off-the-shelf components, an interesting approach has been reported by means of optical invariant analysis [39]. The latter approach depends on the analysis of the optical invariant of a large number of commercially available objectives, relay lenses, mirror scanners, and emission collection systems. The microscope, assembled according to this approach, can image over a  $7\ \text{mm}$  diameter FOV with a  $1.7\ \mu\text{m}$  lateral and  $28\ \mu\text{m}$  axial resolution. Recently, a large FOV has been achieved by merging a sequence of small areas acquired by a rotating micro-opto-mechanical device (capable of laterally translating the imaging area) placed between the objective surface and the imaging plane [40]. Although the development of new optical systems able to provide a large FOV is fundamental whole-brain activity recording, it comes at the cost of a lower temporal resolution, as the scanning of a large area is time consuming. In this framework, a beneficial method for improving wide imaging with enhanced temporal resolution of different regions of the brain is to use a custom multi-area approach. The simplest system that provides simultaneous imaging of two regions of interest is a two-photon microscope that employs two distinct laser beams [41]. The microscope is capable of raster scanning two sub-areas of the brain, enabling independent positioning of the two different laser beams in order to select the appropriate imaging areas. The microscope

has been tested by performing simultaneous calcium imaging across different mouse brain regions during texture discrimination behavior. A similar method has been developed by Stirrman *et al.* [42]. In this case, the researchers reported on a two-photon imaging system that preserves individual neuron resolution across a wide  $9.5\ \text{mm}^2$  FOV and can simultaneously scan neuronal populations over extended cortical networks.

### B. Fast Volumetric Imaging

One of the main challenges in multiphoton microscopy is to increase the volumetric imaging capability while preserving a high spatiotemporal resolution. Owing to the temporal raster-scanning approach of most imaging systems, the acquisition volumetric rate is limited by the extent of the volume sample. As stated above, a large majority of LSMs use galvanometer mirrors and piezo stages for lateral and axial scanning, respectively. Although galvanometric mirrors provide large angular beam deflection and high reflective capability, a significant disadvantage lies in their inertia-limited slow speed. Enhanced fast scanning may be implemented with rotating polygonal mirrors or resonant galvanometers [Fig. 3(c)] [43,44]. However, such scanning systems are limited to raster scanning with fixed scanning speeds and non-homogenous pixel dwell time. Speed constraints are more severe in the axial direction where the inertia of the moving objective limits the axial scanning speed. Piezo stages allow a long axial positioning range (up to  $400\ \mu\text{m}$ ) but suffer from a relatively slow resolving time, especially for large mass objectives. To avoid translation of a highly weighted objective, the imaging plane can be remotely moved by means of a lighter mirror placed in an image-conjugated plane [45,46]. Alternatively, for high-speed volumetric imaging, electrically tunable lenses (ETL) have been demonstrated as a promising technology [47]. ETLs are based on a flexible membrane made by elastic polymer materials that allows fast surface shaping and consequently enhanced focusing capability when coupled to the microscope objective [Fig. 3(d)]. To improve the volumetric acquisition rate, a beneficial and interesting strategy in multiphoton microscopy is the use of multiple planes to parallelize the imaging process. Recently, a novel approach for simultaneously imaging multiple layers of the mouse cortex combined holographic two-photon microscopy with advanced computational methods [48]. The imaging system uses a prior knowledge of neuronal spatial distribution across the cortex and a custom algorithm to extract signals from single neurons from different focal planes acquired simultaneously.

When fast functional imaging of a selected number of neurons within the brain is needed, a fast beam pointer such as an acousto-optic deflector (AOD) can be positively used [49]. In standard raster-scanning approaches, a plane of the sample is continuously scanned, and if the sample is sparsely labelled, significant imaging time is wasted. AODs allow selective access to targeted regions of interest by quickly jumping among different regions [Fig. 3(e)]. In this way, it is possible to increase the imaging speed by up to several orders of magnitude as compared to the raster-scanning approach. However, AOD scanners are highly dispersive devices and suffer from a limited deflection angle. An optimized system with dynamical compensation for optical properties during measurements was demonstrated by accurate modifications of the AOD deflector driver functions [50]. Besides optical and computational corrections, in AOD point recording, any sample motion needs to be closely monitored in order to avoid fluorescence artefacts due to tissue movement in awake imaging. Artefacts have

been reduced by a recent method that quickly moves the excitation spot within a tailored region of interest while continuously recording fluorescence [51]. In this way, it is possible to extend the selected scanning points to cover the neuron's adjacent areas. More recently, a compact AOD microscope for 3D imaging in awake, behaving animals has been reported [52]. On the road to fast 3D imaging, an interesting method for the localization of dispersed neurons is based on the capability to encode the axial localization in a lateral displacement. The encoded approach allows retrieval of 3D information from a 2D image, avoiding the need for slow axial scanning. A volumetric calcium imaging method that uses an elongated V-shaped point spread function to encode the axial position of neurons in a single 2D image has been successfully demonstrated within a 3D brain volume [53]. Finally, it is important to mention that in two-photon microscopy, as in any imaging method, a significant number of photons is necessary for image formation. Optimization of the scanning system at the point spread function level has been demonstrated to improve the collection efficiency and thus the overall volumetric rate. In this framework, a method based on light sculpting has been used in *in vivo* volumetric calcium imaging of a mouse cortical column at single-cell resolution and fast volume rates [54]. This result has been achieved by tailoring the point spread function of the microscope to the structures of interest while maximizing the signal-to-noise ratio. This enabled *in vivo* recording of calcium dynamics of several thousand neurons across cortical layers and in the hippocampus of awake, behaving mice.

### C. Deep Brain Imaging

In scattering tissue such as a mouse brain, the excitation beam is distorted as it propagates in the sample, resulting in a larger point spread function and a decreasing signal-to-background ratio (SBR). This effect limits the imaging depth, even in two-photon microscopy. An approach to monitor neuronal activity in deep brain tissue *in vivo* that does not require optical implementations was developed by Mizrahi and colleagues [55], where the overlying cortex was removed. The same idea was later employed by the Tank Lab, where two-photon imaging was performed in hippocampal and striatal neurons in awake, head-restrained [56–58] mice. Alternatively, simple optical schemes may provide a valid solution for deep brain imaging. Microprisms inserted into the brain provide direct access to targeted deep or difficult to reach brain regions. Though invasive, microprisms allow simultaneous visualization of all cortical layers and investigation of inter- and intralaminar cortical dynamics [59–62] [Fig. 4(a)]. In addition, multiphoton endoscopy exploits the insertion of a gradient-index (GRIN) lens to directly access deep brain structures [Fig. 4(b)]. After the proof-of-principle study of Jung and Schnitzel in 2003 [63], the system was first applied *in vivo* by Levene and colleagues [64]. GRIN lenses were later customized to perform high-resolution imaging of dendritic spines in the CA1 hippocampus by Attardo and colleagues [65]. While these insertion approaches can monitor activity in freely moving animals over long periods [66,67], they are highly invasive and are typically limited to a single and somewhat narrow FOV.

Even though two-photon excitation microscopy combined with specialized optics helps us to reach deeper layers *in vivo* by minimizing the thickness of the brain tissue to cross, it does not solve the problem of light scattering, which fundamentally limits the imaging depth in highly scattering biological specimens [68].

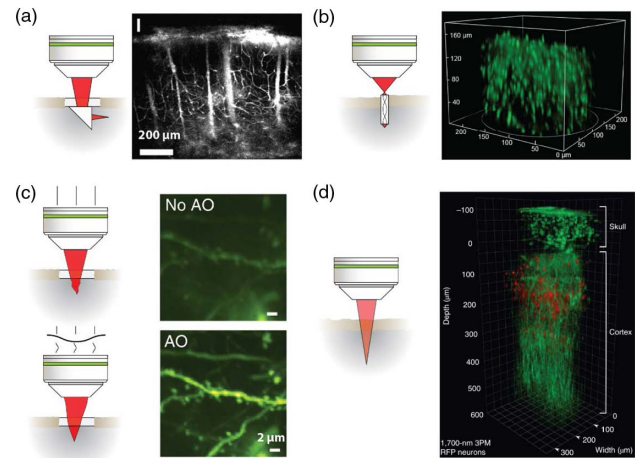


**Fig. 4.** Deep brain imaging. (a) Left: scheme of microprism implantation. Right: Simultaneous imaging of all cortical layers through invasive microprism, adapted by permission from American Physiological Society [60], scale bar 200  $\mu\text{m}$ . (b) Left: GRIN lens optical scheme; right: deep brain imaging of freely behaving mouse via a GRIN lens miniaturized microscope, adapted from [67]. (c) Left: schematic of wavefront correction of the signal coming from a deep region of the scattering sample; brain imaging adapted by permission from Springer Nature [77]. (d) Three-photon microscopy through the skull of a mouse, adapted by permission from Springer Nature [91].

Simultaneous spatial and temporal focusing of femtosecond pulses [69,70] has great potential to optimize the point spread function to sample spatial distribution. Temporal focusing was first demonstrated by Tal and colleagues [71] and later applied to the central nervous system of *elegans* to achieve near-simultaneous activity recording of most of the head neurons [72]. Nevertheless, temporal focusing implies a spatially delocalized excitation, which requires image formation, not fully exploiting the advantages of two-photon microscopy. Therefore, the main application for this tool consists of light-patterning for photostimulation [73,74]. In addition, temporal focusing does not solve the distortion of the excitation beam. Recent work in optics helped to account for substantial optical scattering by developing “wavefront engineering” tools able to extend the depth and accuracy of neurophotonic experiments within tissue [75,76]. The basic idea of adaptive optics is to introduce a distortion to the light wavefront of opposite sign to that generated by the scattering tissue. It is possible to reverse the effects of scattering in a non-invasive manner to maintain micrometer-scale resolution by correcting the spatial phase profile of multiply scattered light exiting from the tissue. Direct [77] or indirect wavefront sensing [78–80] can be used to measure how much the wavefront is distorted by the sample, which is necessary to calculate the distortion pattern. Wavefront engineering can be done with spatial light modulators (SLMs) [77], deformable mirrors [77,80–82], or AODs [83]. Using adaptive optics, fine structures can be resolved in deep layers with an increased signal-to-noise ratio [84,85] [Fig. 4(c)].

Recently, an alternative approach to increase penetration depth took advantage of the decrease in light scattering with increasing wavelength. By using 1100 nm infrared light in combination with redshifted calcium indicators, Kondo and colleagues detected neural activity up to 1200  $\mu\text{m}$  from the cortical surface in the intact mouse brain. By using this approach, the authors could image the entire medial prefrontal cortex and the hippocampal CA1 region of a young mouse (up to four weeks old) [86].

However, a longer excitation wavelength alone is not sufficient to overcome the depth limit imposed by two-photon microscopy due to an out-of-focus background. Three-photon excitation can overcome this limit thanks to strongest localization of excitation along the  $z$  axis (fourth power instead of quadratic extinction) [31–33,87,88]. Thanks to the third-order nonlinearity, three-photon excitation allows us to reach subcortical regions while maintaining high contrast and subcellular resolution in structural and functional studies [89,90]. Furthermore, commonly available fluorescent indicators that with one-photon excitation are excited in the visible range can be excited at three-photon excitation by 1.3–1.7  $\mu\text{m}$  light and thus overcome the lack of fluorescent indicators in the IR excitation window. Finally, IR light was used by Wang *et al.* [91] to demonstrate three-photon imaging of vasculature and calcium imaging of neuronal activity through the adult mouse skull over weeks up to cortical layer 4 in awake mice with a FOV spanning hundreds of micrometers [Fig. 4(d)]. More recently, volumetric three-photon calcium imaging of the hippocampus through an intact cortex of over ten thousand neurons was reported by Vaziri Lab [92]. A limiting drawback of three-photon imaging could lie in the phototoxicity produced by the higher laser power required to excite the fluorophore. Provided a better characterization of this negative aspect, recent three-photon advancements could pave the way to a very non-invasive approach for brain imaging *in vivo*.

#### 4. CONCLUSION

Development of advanced optical methods led to a revolution in neuroscience, allowing registration of neuronal activity across large areas (up to the whole vertebrate brain) deep inside the mammalian brain with high spatiotemporal resolution and in a non-invasive fashion. In this work, we provided a brief overview of the main progress in the field of linear and nonlinear optical imaging, highlighting the relative merits and limitations of different approaches. What is next? One great challenge is to extend the applicability of optical methods to more complex brains. This goal could be achieved by optimizing the existing tools and combining different techniques. For instance, we envision that a combination of three-photon microscopy with wavefront shaping will enable targeting deeper neurons even in non-human primate brains. Another challenge linked to the previous one is the capability of extracting the highest possible number of single-cell functional traces from limited raw data. In this respect, one may expand existing computational approaches that allow disentangling single-neuron activity based on the statistical independence of distinct cells [29,93,94]. In general, the best usage of acquired data is a fundamental issue that is arising across multiple fields of microscopy. The wealth of information hidden inside raw images needs to be carefully treated and extracted to improve our understanding of the brain. In this respect, we believe that artificial intelligence methods—in particular, deep learning—will play a significant role in the future. The potential of artificial intelligence is by no means limited to image processing but could also be exploited in microscope control, for instance, by finding the best scanning strategies in a sample-specific way.

**Funding.** Horizon 2020 Framework Programme (H2020) (654148, 720270, 785907); H2020 Excellent Science—European Research Council (ERC) (692943).

#### REFERENCES

1. M. H. Mohajerani, A. W. Chan, M. Mohsenvand, J. Ledue, R. Liu, D. A. McVea, J. D. Boyd, Y. T. Wang, M. Reimers, and T. H. Murphy, "Spontaneous cortical activity alternates between motifs defined by regional axonal projections," *Nat. Neurosci.* **16**, 1426–1435 (2013).
2. D. Xiao, M. P. Vanni, C. C. Mitelut, A. W. Chan, J. M. Ledue, Y. Xie, A. C. N. Chen, N. V. Swindale, and T. H. Murphy, "Mapping cortical mesoscopic networks of single spiking cortical or sub-cortical neurons," *Elife* **6**, e19976 (2017).
3. M. P. Vanni and T. H. Murphy, "Mesoscale transcranial spontaneous activity mapping in GCaMP3 transgenic mice reveals extensive reciprocal connections between areas of somatomotor cortex," *J. Neurosci.* **34**, 15931–15946 (2014).
4. Y. Hayashi, S. Yawata, K. Funabiki, and T. Hikida, "In vivo calcium imaging from dentate granule cells with wide-field fluorescence microscopy," *PLoS One* **12**, e0180452 (2017).
5. I. Ferezou, F. Haiss, L. J. Gentet, R. Aronoff, B. Weber, and C. C. H. Petersen, "Spatiotemporal dynamics of cortical sensorimotor integration in behaving mice," *Neuron* **56**, 907–923 (2007).
6. K. K. Ghosh, L. D. Burns, E. D. Cocker, A. Nimmerjahn, Y. Ziv, A. El Gamal, and M. J. Schnitzer, "Miniaturized integration of a fluorescence microscope," *Nat. Methods* **8**, 871–878 (2011).
7. J. H. Jennings, R. L. Ung, S. L. Resendez, A. M. Stamatakis, J. G. Taylor, J. Huang, K. Veleta, P. A. Kantak, M. Aita, K. Shilling-Scriver, C. Ramakrishnan, K. Deisseroth, S. Otte, and G. D. Stuber, "Visualizing hypothalamic network dynamics for appetitive and consummatory behaviors," *Cell* **160**, 516–527 (2015).
8. Y. Ziv, L. D. Burns, E. D. Cocker, E. O. Hamel, K. K. Ghosh, L. J. Kitch, A. El Gamal, and M. J. Schnitzer, "Long-term dynamics of CA1 hippocampal place codes," *Nat. Neurosci.* **16**, 264–266 (2013).
9. L. Turrini, C. Fometto, G. Marchetto, M. C. Müllenbroich, N. Tiso, A. Vettori, F. Resta, A. Masi, G. Mannaioni, F. S. Pavone, and F. Vanzi, "Optical mapping of neuronal activity during seizures in zebrafish," *Sci. Rep.* **7**, 3025 (2017).
10. D. H. Kim, J. Kim, J. C. Marques, A. Grama, D. G. C. Hildebrand, W. Gu, J. M. Li, and D. N. Robson, "Pan-neuronal calcium imaging with cellular resolution in freely swimming zebrafish," *Nat. Methods* **14**, 1107–1114 (2017).
11. P. Symvoulidis, A. Lauri, A. Stefanou, M. Cappetta, S. Schneider, H. Jia, A. Stelzl, M. Koch, C. C. Perez, A. Myklatun, S. Renninger, A. Chmyrov, T. Lasser, W. Wurst, V. Ntziachristos, and G. G. Westmeyer, "NeuTracker—imaging neurobehavioral dynamics in freely behaving fish," *Nat. Methods* **14**, 1079–1082 (2017).
12. R. M. Power and J. Huisken, "A guide to light-sheet fluorescence microscopy for multiscale imaging," *Nat. Methods* **14**, 360–373 (2017).
13. M. B. Ahrens, M. B. Orger, D. N. Robson, J. M. Li, and P. J. Keller, "Whole-brain functional imaging at cellular resolution using light-sheet microscopy," *Nat. Methods* **10**, 413–420 (2013).
14. T. Panier, S. A. Romano, R. Olive, T. Pietri, G. Sumbre, R. Candelier, and G. Debrégeas, "Fast functional imaging of multiple brain regions in intact zebrafish larvae using selective plane illumination microscopy," *Front. Neural Circuits* **7**, 65 (2013).
15. L. A. Royer, W. C. Lemon, R. K. Chhetri, Y. Wan, M. Coleman, E. W. Myers, and P. J. Keller, "Adaptive light-sheet microscopy for long-term, high-resolution imaging in living organisms," *Nat. Biotechnol.* **34**, 1267–1278 (2016).
16. M. C. Müllenbroich, L. Turrini, L. Silvestri, T. Alterini, A. Gheisari, F. Vanzi, L. Sacconi, and F. S. Pavone, "Bessel beam illumination reduces random and systematic errors in quantitative functional studies using light-sheet microscopy," *Front. Cell. Neurosci.* **12**, 1–12 (2018).
17. G. Sancataldo, V. Gavryusev, G. de Vito, L. Turrini, M. Locatelli, C. Fometto, N. Tiso, F. Vanzi, L. Silvestri, and F. S. Pavone, "Flexible multi-beam light-sheet fluorescence microscope for live imaging without striping artifacts," *Front. Neuroanat.* **13**, 7 (2019).
18. M. A. Taylor, G. C. Vanwallendael, I. A. Favre-Bulle, and E. K. Scott, "Diffuse light-sheet microscopy for stripe-free calcium imaging of neural populations," *J. Biophoton.* **11**, e201800088 (2018).
19. N. Vladimirov, Y. Mu, T. Kawashima, D. V. Bennett, C. T. Yang, L. L. Looger, P. J. Keller, J. Freeman, and M. B. Ahrens, "Light-sheet functional imaging in fictively behaving zebrafish," *Nat. Methods* **11**, 883–884 (2014).

20. S. Wolf, W. Supatto, G. Debrégeas, P. Mahou, S. G. Kruglik, J. M. Sintes, E. Beaurepaire, and R. Candelier, "Whole-brain functional imaging with two-photon light-sheet microscopy," *Nat. Methods* **12**, 379–380 (2015).
21. R. Tomer, M. Lovett-Barron, I. Kauvar, A. Andalman, V. M. Burns, S. Sankaran, L. Grosenick, M. Broxton, S. Yang, and K. Deisseroth, "SPED light sheet microscopy: fast mapping of biological system structure and function," *Cell* **163**, 1796–1806 (2015).
22. S. Quirin, N. Vladimirov, C.-T. Yang, D. S. Peterka, R. Yuste, and M. B. Ahrens, "Calcium imaging of neural circuits with extended depth-of-field light-sheet microscopy," *Opt. Lett.* **41**, 855 (2016).
23. M. Levoy, R. Ng, A. Adams, M. Footer, and M. Horowitz, "Light field microscopy," *ACM Trans. Graph.* **25**, 924–934 (2006).
24. R. Prevedel, Y. G. Yoon, M. Hoffmann, N. Pak, G. Wetzstein, S. Kato, T. Schrödel, R. Raskar, M. Zimmer, E. S. Boyden, and A. Vaziri, "Simultaneous whole-animal 3D imaging of neuronal activity using light-field microscopy," *Nat. Methods* **11**, 727–730 (2014).
25. N. C. Pégard, H.-Y. Liu, N. Antipa, M. Gerlock, H. Adesnik, and L. Waller, "Compressive light-field microscopy for 3D neural activity recording," *Optica* **3**, 517–524 (2016).
26. M. A. Taylor, T. Nöbauer, A. Pernia-Andrade, F. Schlumm, and A. Vaziri, "Brain-wide 3D light-field imaging of neuronal activity with speckle-enhanced resolution," *Optica* **5**, 345–353 (2018).
27. T. F. Holekamp, D. Turaga, and T. E. Holy, "Fast three-dimensional fluorescence imaging of activity in neural populations by objective-coupled planar illumination microscopy," *Neuron* **57**, 661–672 (2008).
28. M. B. Bouchard, V. Voleti, C. S. Mendes, C. Lacefield, W. B. Grueber, R. S. Mann, R. M. Bruno, and E. M. C. Hillman, "Swept confocally-aligned planar excitation (SCAPE) microscopy for high-speed volumetric imaging of behaving organisms," *Nat. Photonics* **9**, 113–119 (2015).
29. T. Nöbauer, O. Skocek, A. J. Pernia-Andrade, L. Weillguny, F. Martínez Traub, M. I. Molodtsov, and A. Vaziri, "Video rate volumetric Ca<sup>2+</sup> imaging across cortex using seeded iterative demixing (SID) microscopy," *Nat. Methods* **14**, 811–818 (2017).
30. W. Denk, J. H. Strickler, and W. W. Webb, "Two-photon laser scanning fluorescence microscopy," *Science* **248**, 73–76 (1990).
31. P. T. So, "Two-photon fluorescence light microscopy," in *ELS* (Wiley, 2001), <https://doi.org/10.1038/npg.els.0002991>.
32. W. R. Zipfel, R. M. Williams, and W. W. Webb, "Nonlinear magic: multiphoton microscopy in the biosciences," *Nat. Biotechnol.* **21**, 1369–1377 (2003).
33. T. W. Chen, T. J. Wardill, Y. Sun, S. R. Pulver, S. L. Renninger, A. Baohan, E. R. Schreiter, R. A. Kerr, M. B. Orger, V. Jayaraman, L. L. Looger, K. Svoboda, and D. S. Kim, "Ultrasensitive fluorescent proteins for imaging neuronal activity," *Nature* **499**, 295–300 (2013).
34. M. Z. Lin and M. J. Schnitzer, "Genetically encoded indicators of neuronal activity," *Nat. Neurosci.* **19**, 1142–1153 (2016).
35. C. Deo and L. D. Lavis, "Synthetic and genetically encoded fluorescent neural activity indicators," *Curr. Opin. Neurobiol.* **50**, 101–108 (2018).
36. A. Ustione and D. W. Piston, "A simple introduction to multiphoton microscopy," *J. Microsc.* **243**, 221–226 (2011).
37. N. J. Sofroniew, D. Flickinger, J. King, and K. Svoboda, "A large field of view two-photon mesoscope with subcellular resolution for in vivo imaging," *Elife* **5**, e14472 (2016).
38. P. S. Tsai, C. Mateo, J. J. Field, C. B. Schaffer, M. E. Anderson, and D. Kleinfeld, "Ultra-large field-of-view two-photon microscopy," *Opt. Express* **23**, 13833–13847 (2015).
39. J. R. Bumstead, "Designing a large field-of-view two-photon microscope using optical invariant analysis," *Neurophotonics* **5**, 1 (2018).
40. S. I. Terada, K. Kobayashi, M. Ohkura, J. Nakai, and M. Matsuzaki, "Super-wide-field two-photon imaging with a micro-optical device moving in post-objective space," *Nat. Commun.* **9**, 3550 (2018).
41. J. L. Chen, F. F. Voigt, M. Javadzadeh, R. Krueppel, and F. Helmchen, "Long-range population dynamics of anatomically defined neocortical networks," *Elife* **5**, e14679 (2016).
42. J. N. Stirman, I. T. Smith, M. W. Kudenov, and S. L. Smith, "Wide field-of-view, multi-region, two-photon imaging of neuronal activity in the mammalian brain," *Nat. Biotechnol.* **34**, 857–862 (2016).
43. K. H. Kim, C. Buehler, and P. T. C. So, "High-speed, two-photon scanning microscope," *Appl. Opt.* **38**, 6004–6009 (1999).
44. Q. T. Nguyen, N. Callamaras, C. Hsieh, and I. Parker, "Construction of a two-photon microscope for video-rate Ca<sup>2+</sup>-imaging," *Cell Calcium* **30**, 383–393 (2001).
45. E. J. Botcherby, R. Juškaitis, M. J. Booth, and T. Wilson, "An optical technique for remote focusing in microscopy," *Opt. Commun.* **281**, 880–887 (2008).
46. F. Anselmi, C. Ventalon, A. Begue, D. Ogden, and V. Emiliani, "Three-dimensional imaging and photostimulation by remote-focusing and holographic light patterning," *Proc. Natl. Acad. Sci. USA* **108**, 19504–19509 (2011).
47. B. F. Grewe, F. F. Voigt, M. van't Hoff, and F. Helmchen, "Fast two-layer two-photon imaging of neuronal cell populations using an electrically tunable lens," *Biomed. Opt. Express* **2**, 2035–2046 (2011).
48. W. Yang, J. K. Miller, L. Carrillo-Reid, E. Pneumatikakis, L. Paninski, R. Yuste, and D. S. Peterka, "Simultaneous multi-plane imaging of neural circuits," *Neuron* **89**, 269–284 (2016).
49. G. D. Reddy and P. Saggau, "Fast three-dimensional laser scanning scheme using acousto-optic deflectors," *J. Biomed. Opt.* **10**, 064038 (2005).
50. G. Katona, G. Szalay, P. Maák, A. Kaszás, M. Veress, D. Hillier, B. Chiovini, E. S. Vizi, B. Roska, and B. Rózsa, "Fast two-photon in vivo imaging with three-dimensional random-access scanning in large tissue volumes," *Nat. Methods* **9**, 201–208 (2012).
51. G. Szalay, L. Judák, G. Katona, K. Ócsai, G. Juhász, M. Veress, Z. Szadai, A. Fehér, T. Tompa, B. Chiovini, P. Maák, and B. Rózsa, "Fast 3D imaging of spine, dendritic, and neuronal assemblies in behaving animals," *Neuron* **92**, 723–738 (2016).
52. K. M. N. S. Nadella, H. Roš, C. Baragli, V. A. Griffiths, G. Konstantinou, T. Koimtzis, G. J. Evans, P. A. Kirkby, and R. A. Silver, "Random-access scanning microscopy for 3D imaging in awake behaving animals," *Nat. Methods* **13**, 1001–1004 (2016).
53. A. Song, A. S. Charles, S. A. Koay, J. L. Gauthier, S. Y. Thiberge, J. W. Pillow, and D. W. Tank, "Volumetric two-photon imaging of neurons using stereoscopy (vTwINS)," *Nat. Methods* **14**, 420–426 (2017).
54. R. Prevedel, A. J. Verhoef, A. J. Pernia-Andrade, S. Weisenburger, B. S. Huang, T. Nöbauer, A. Fernández, J. E. Delcour, P. Golshani, A. Baltuska, and A. Vaziri, "Fast volumetric calcium imaging across multiple cortical layers using sculpted light," *Nat. Methods* **13**, 1021–1028 (2016).
55. A. Mizrahi, C. J. Crowley, E. Shtoyerman, and L. C. Katz, "High-resolution in vivo imaging of hippocampal dendrites and spines," *J. Neurosci.* **24**, 3147–3151 (2004).
56. D. A. Dombeck, C. D. Harvey, L. Tian, L. L. Looger, and D. W. Tank, "Functional imaging of hippocampal place cells at cellular resolution during virtual navigation," *Nat. Neurosci.* **13**, 1433–1440 (2010).
57. M. W. Howe and D. A. Dombeck, "Rapid signalling in distinct dopaminergic axons during locomotion and reward," *Nature* **535**, 505–510 (2016).
58. M. E. J. Sheffield and D. A. Dombeck, "Calcium transient prevalence across the dendritic arbour predicts place field properties," *Nature* **517**, 200–204 (2015).
59. R. J. Low, Y. Gu, and D. W. Tank, "Cellular resolution optical access to brain regions in fissures: imaging medial prefrontal cortex and grid cells in entorhinal cortex," *Proc. Natl. Acad. Sci. USA* **111**, 18739–18744 (2014).
60. T. H. Chia and M. J. Levene, "Microprisms for in vivo multilayer cortical imaging," *J. Neurophysiol.* **102**, 1310–1314 (2009).
61. J. G. Heys, K. V. Rangarajan, and D. A. Dombeck, "The functional micro-organization of grid cells revealed by cellular-resolution imaging," *Neuron* **84**, 1079–1090 (2014).
62. M. L. Andermann, N. B. Gilfoy, G. J. Goldey, R. N. S. Sachdev, M. Wölfel, D. A. McCormick, R. C. Reid, and M. J. Levene, "Chronic cellular imaging of entire cortical columns in awake mice using microprisms," *Neuron* **80**, 900–913 (2013).
63. J. C. Jung and M. J. Schnitzer, "Multiphoton endoscopy," *Opt. Lett.* **28**, 902–904 (2003).
64. M. J. Levene, D. A. Dombeck, K. A. Kasischke, R. P. Molloy, and W. W. Webb, "In vivo multiphoton microscopy of deep brain tissue," *J. Neurophysiol.* **91**, 1908–1912 (2004).
65. A. Attardo, J. E. Fitzgerald, and M. J. Schnitzer, "Impermanence of dendritic spines in live adult CA1 hippocampus," *Nature* **523**, 592–596 (2015).
66. R. P. J. Barretto, T. H. Ko, J. C. Jung, T. J. Wang, G. Capps, A. C. Waters, Y. Ziv, A. Attardo, L. Recht, and M. J. Schnitzer, "Time-lapse imaging of disease progression in deep brain areas using fluorescence microendoscopy," *Nat. Med.* **17**, 223–228 (2011).
67. B. N. Ozbay, G. L. Futia, M. Ma, V. M. Bright, J. T. Gopinath, E. G. Hughes, D. Restrepo, and E. A. Gibson, "Three dimensional two-photon brain imaging in freely moving mice using a miniature fiber coupled microscope with active axial-scanning," *Sci. Rep.* **8**, 8108 (2018).

68. F. Helmchen and W. Denk, "Deep tissue two-photon microscopy," *Nat. Methods* **2**, 932–940 (2005).
69. G. Zhu, J. van Howe, M. Durst, W. Zipfel, and C. Xu, "Simultaneous spatial and temporal focusing of femtosecond pulses," *Opt. Express* **13**, 2153–2159 (2005).
70. D. Oron and Y. Silberberg, "Temporal focusing microscopy," *Cold Spring Harbor Protocols* **2015**, 145–151 (2015).
71. E. Tal, D. Oron, and Y. Silberberg, "Improved depth resolution in video-rate line-scanning multiphoton microscopy using temporal focusing," *Opt. Lett.* **30**, 1686–1688 (2005).
72. T. Schrödel, R. Prevedel, K. Aumayr, M. Zimmer, and A. Vaziri, "Brain-wide 3D imaging of neuronal activity in *Caenorhabditis elegans* with sculpted light," *Nat. Methods* **10**, 1013–1020 (2013).
73. O. A. Shemesh, D. Tanese, V. Zampini, C. Linghu, K. Piatkevich, E. Ronzitti, E. Papagiakoumou, E. S. Boyden, and V. Emiliani, "Temporally precise single-cell-resolution optogenetics," *Nat. Neurosci.* **20**, 1796–1806 (2017).
74. O. Hernandez, E. Papagiakoumou, D. Tanese, K. Fidelin, C. Wyart, and V. Emiliani, "Three-dimensional spatiotemporal focusing of holographic patterns," *Nat. Commun.* **7**, 11928 (2016).
75. R. Horstmeyer, H. Ruan, and C. Yang, "Guidestar-assisted wavefront-shaping methods for focusing light into biological tissue," *Nat. Photonics* **9**, 563–571 (2015).
76. N. Ji, "Adaptive optical fluorescence microscopy," *Nat. Methods* **14**, 374–380 (2017).
77. K. Wang, D. E. Milkie, A. Saxena, P. Engerer, T. Misgeld, M. E. Bronner, J. Mumm, and E. Betzig, "Rapid adaptive optical recovery of optimal resolution over large volumes," *Nat. Methods* **11**, 625–628 (2014).
78. N. Ji, D. E. Milkie, and E. Betzig, "Adaptive optics via pupil segmentation for high-resolution imaging in biological tissues," *Nat. Methods* **7**, 141–147 (2010).
79. D. Debarre, M. J. Booth, and T. Wilson, "Image based adaptive optics through optimisation of low spatial frequencies," *Opt. Express* **15**, 8176–8190 (2007).
80. D. Débarre, E. J. Botcherby, T. Watanabe, S. Srinivas, M. J. Booth, and T. Wilson, "Image-based adaptive optics for two-photon microscopy," *Opt. Lett.* **34**, 2495–2497 (2009).
81. M. A. A. Neil, M. J. Booth, and T. Wilson, "New modal wave-front sensor: a theoretical analysis," *J. Opt. Soc. Am. A* **17**, 1098–1107 (2000).
82. M. Rueckel, J. A. Mack-Bucher, and W. Denk, "Adaptive wavefront correction in two-photon microscopy using coherence-gated wavefront sensing," *Proc. Natl. Acad. Sci. USA* **103**, 17137–17142 (2006).
83. W. Akemann, J.-F. Léger, C. Ventalon, B. Mathieu, S. Dieudonné, and L. Bourdieu, "Fast spatial beam shaping by acousto-optic diffraction for 3D non-linear microscopy," *Opt. Express* **23**, 28191–28205 (2015).
84. W. Sun, Z. Tan, B. D. Mensh, and N. Ji, "Thalamus provides layer 4 of primary visual cortex with orientation- and direction-tuned inputs," *Nat. Neurosci.* **19**, 308–315 (2016).
85. C. Wang, R. Liu, D. E. Milkie, W. Sun, Z. Tan, A. Kerlin, T. W. Chen, D. S. Kim, and N. Ji, "Multiplexed aberration measurement for deep tissue imaging in vivo," *Nat. Methods* **11**, 1037–1040 (2014).
86. M. Kondo, K. Kobayashi, M. Ohkura, J. Nakai, and M. Matsuzaki, "Two-photon calcium imaging of the medial prefrontal cortex and hippocampus without cortical invasion," *Elife* **6**, e26839 (2017).
87. C. Xu, W. Zipfel, J. B. Shear, R. M. Williams, and W. W. Webb, "Multiphoton fluorescence excitation: new spectral windows for biological nonlinear microscopy," *Proc. Natl. Acad. Sci. USA* **93**, 10763–10768 (1996).
88. D. L. Wokosin, V. E. Centonze, S. Crittenden, and J. White, "Three-photon excitation fluorescence imaging of biological specimens using an all-solid-state laser," *Bioimaging* **4**, 208–214 (1996).
89. N. G. Horton, K. Wang, D. Kobat, C. G. Clark, F. W. Wise, C. B. Schaffer, and C. Xu, "In vivo three-photon microscopy of subcortical structures within an intact mouse brain," *Nat. Photonics* **7**, 205–209 (2013).
90. D. G. Ouzounov, T. Wang, M. Wang, D. D. Feng, N. G. Horton, J. C. Cruz-Hernández, Y. T. Cheng, J. Reimer, A. S. Tolias, N. Nishimura, and C. Xu, "In vivo three-photon imaging of activity of Gcamp6-labeled neurons deep in intact mouse brain," *Nat. Methods* **14**, 388–390 (2017).
91. T. Wang, D. G. Ouzounov, C. Wu, N. G. Horton, B. Zhang, C. H. Wu, Y. Zhang, M. J. Schnitzer, and C. Xu, "Three-photon imaging of mouse brain structure and function through the intact skull," *Nat. Methods* **15**, 789–792 (2018).
92. S. Weisenburger, F. Tejera, J. Demas, B. Chen, J. Manley, F. T. Sparks, F. Martínez Traub, T. Daigle, H. Zeng, A. Losonczy, and A. Vaziri, "Volumetric Ca<sup>2+</sup> imaging in the mouse brain using hybrid multiplexed sculpted light microscopy," *Cell* **177**, 1–17 (2019).
93. L. Theis, P. Berens, E. Froudarakis, J. Reimer, M. Román Rosón, T. Baden, T. Euler, A. S. Tolias, and M. Bethge, "Benchmarking spike rate inference in population calcium imaging," *Neuron* **90**, 471–482 (2016).
94. E. A. Pnevmatikakis, D. Soudry, Y. Gao, T. A. Machado, J. Merel, D. Pfau, T. Reardon, Y. Mu, C. Lacefield, W. Yang, M. Ahrens, R. Bruno, T. M. Jessell, D. S. Peterka, R. Yuste, and L. Paninski, "Simultaneous denoising, deconvolution, and demixing of calcium imaging data," *Neuron* **89**, 285–299 (2016).